PRAMANA
— journal of
physics

Vol. 57, No. 4
October 2001
pp. 795–808

Theory of anisotropic diamagnetism, local moment magnetization and carrier spin-polarization in $Pb_{1-x}Eu_xTe$

R C PATNAIK, R K DAS[1], R L HOTA[2] and G S TRIPATHI[3]
Department of Physics, S.K.C.G College, Parlakhemundi 761 200, India
[1]Department of Physics, Gopalpur College, Gopalpur 761 002, India
[2]Department of Physics, Jagannath Institute for Technology and Management, Parlakhemundi 761 211, India
[3]Department of Physics, Berhampur University, Berhampur 760 007, India

MS received 16 October 2000; revised 1 March 2001

Abstract. We present theoretical analyses of anisotropic lattice diamagnetism, magnetization due to magnetic ions and carrier spin-polarization in the diluted magnetic semiconductor, $Pb_{1-x}Eu_xTe$. The lattice diamagnetism results from orbital susceptibility due to inter band effects and spin-orbit contributions. The spin-orbit contribution is found to be dominant. However, both the contributions show pronounced anisotropy. With increase in x, the diamagnetism decreases. We consider contributions from randomly distributed isolated magnetic ions and clusters of pairs and triads for the local moment magnetization. The isolated magnetic-ion contribution is the dominant one. We calculate the magnetization for two typical magnetic ion concentrations: $x = 0.03$ and $x = 0.06$. Temperature dependence of the magnetization is also considered. Apart from lattice and localized magnetic ions, the carrier contribution to the spin-density is also calculated for a carrier density of $p = 10^{18}$ cm^{-3}. The relative spin-density of carriers increases with increase in the magnetic field strength and magnetic ion concentration. The agreement with experiment where available is reasonably good.

Keywords. Orbital diamagnetism; magnetization; sp-f hybridization; spin density; diluted magnetic semiconductors.

PACS Nos 75.50 Pp; 75.20 Ck; 75.10 Lp

1. Introduction

The physics of magnetic impurities in non-magnetic metals abounds in richness and complexity of phenomena and has been studied for decades. In contrast, magnetic impurity problem in semiconductors is relatively a new subject [1–3]. The study involving the interplay between magnetism and semiconductor physics was not pursued seriously in the past partly due to the belief that, unlike metals, semiconductors were never considered as important materials for magnetic applications and to the fact that the quantum theory (which is inevitable for studying magnetism) of semiconductors was not as appealing and fascinating as it is for metals. However, during the last one and half decades the physics of a class of magnetic materials known as diluted magnetic semiconductors (DMS) is found

to be, if not more, at least as interesting as that in 'diluted-magnetic metals'. The DMS are normally based on II–VI or IV–VI semiconductors and magnetic ions which exist in dilute limits replacing the host cations are either transition element ions or rare earth ones. The list of such materials can be had from recent review articles [1,3]. Compared to II–VI based DMS, the research work done on IV–VI based DMS has been substantially less. Furthermore, although there has been considerable activity in the experimental aspects [4–6] of different magnetic properties of these systems, it has not been adequately matched by theoretical work. The IV–VI based DMS, $Pb_{1-x}Eu_xTe$ constitutes an interesting material in the sense that the host material PbTe is a degenerate semiconductor, thus partly behaving like a metal without, in any way, losing its principal semiconducting characteristics. A typical DMS is formed by two subsystems – a subsystem of magnetic ions and the surrounding electronic environment. Depending on the nature of the investigation, these two subsystems can either be treated separately or simultaneously via the hybridization of carriers and the local moments. We have recently calculated within the effective mass representation (EMR) [7] the effective g-factors and effective masses of $Pb_{1-x}Eu_xTe$ [8]. These calculations reveal interesting anisotropic effects in this system. These are basically electronic quantities and the effects of magnetic ions are studied through the aforesaid hybridization.

As a continuation of our research in this system, we present here detailed analyses of different magnetic properties of $Pb_{1-x}Eu_xTe$ in three parts. In §2, we calculate the lattice diamagnetic susceptibility, by assuming the valence band full and the conduction band empty. The effect of magnetic ions is considered only through the changes in the energy gap. In §3, the magnetization due to the local magnetic ions is considered from single magnetic ions and clusters of pairs and triads. We consider the hybridization of these two subsystems and calculate its effect on the spin-density of carriers in §4. Thus the magnetic properties of all the constituents of the system are considered. This is done for the first time in this system theoretically, and the work reveals interesting physics. We summarize our results in §5.

2. Anisotropic lattice diamagnetism

There are very few subjects in magnetism which are as tough as the orbital magnetic susceptibility of Bloch electrons. Although it has occupied many theorists during the last four decades (see for example Tripathi [9] and Enz [10] for references) calculation of the orbital susceptibility for a real system has always been a daunting exercise because of the enormous complexity associated with the problem. $Pb_{1-x}Eu_xTe$ is a multiband system with pronounced effects arising from spin–orbit interaction. The expression for the magnetic susceptibility (χ) of Bloch electrons in the presence of magnetic impurities and spin–orbit interaction is written as [9]

$$\chi = \chi_{\mathrm{MK}} + \chi_{\mathrm{loc}}, \tag{2.1}$$

where χ_{MK} is the magnetic susceptibility of Bloch electrons derived by Misra and Kleinman [11] and χ_{loc} is the contribution due to the hybridization of a conduction electron with the magnetic impurities. Since the lattice diamagnetism arises from the electrons in a full valence band, the second term is not considered in evaluating χ_{dia}, the diamagnetic susceptibility. The effect of magnetic impurities is considered here via the modification of the electronic structure. Thus, in what follows, we use χ_{MK} for the evaluation of the lattice

diamagnetism, which is expressed as a sum of spin, orbital and spin–orbit contributions. Since the spin susceptibility and the Landau–Peierls contribution to the orbital susceptibility are zero for a full valence band, the modified χ_{MK} in the absence of these contributions can be written as

$$\chi_{\mathrm{MK}}^{\mathrm{dia}} = \chi_{ibo} + \chi_{so}, \tag{2.2}$$

where χ_{ibo} is the interband contribution to the orbital magnetic susceptibility which is obtained by subtracting the χ_{LP} (Landau–Peierls susceptibility) from χ_o, obtained by Misra and Kleinman [11], and χ_{so} is the spin–orbit contribution to the susceptibility.

A. *Calculational procedure*

The host system PbTe is described by six energy levels at the L-point of the Brillouin zone [12]. The energy gap E_g is a direct one, about 0.19 eV and changes as a function of magnetic ion concentration [13,14]. The Hamiltonians for the band edge states are diagonalized exactly and the effects of far bands are considered using $\vec{k}\cdot\vec{\pi}$ perturbation theory in the EMR. $\vec{\pi}$ is the momentum operator in the presence of the spin–orbit interaction. The mathematical details of this procedure are described in our earlier work [15,16].

When the field is along the z-direction [001], the magnetic susceptibility is given by

$$\chi_{\mathrm{dia}} = 4\left(\frac{1}{3}\chi^{l} + \frac{2}{3}\chi^{t}\right), \tag{2.3}$$

where l and t are along crystallographic [111] and $[\overline{11}2]$ or $[1\bar{1}0]$ respectively. Here the factor four appears because of four equivalent L points in the Brillouin zone and

$$\chi^{l,t} = \chi_{ibo}^{l,t} + \chi_{so}^{l,t} \tag{2.4}$$

and the expressions for $\chi_{ibo}^{l,t}$ and $\chi_{so}^{l,t}$ are obtained by summing the $\vec{k}$-dependent parts of $\chi_{ibo}^{l,t}(\vec{k})$ and $\chi_{so}^{l,t}(\vec{k})$ [11] over all $\vec{k}$'s in the Brillouin zone. These are derived after tedious algebra and expressed as

$$\chi_{ibo}^{l}(\vec{k}) = -2\frac{e^2s^2}{mc^2E_g^2W^2}\left[1 - \frac{\hbar^2}{m^2}\frac{s^2(k_x^2+k_y^2)}{E_g^2W^2}\right], \tag{2.5}$$

$$\chi_{ibo}^{t}(\vec{k}) = -2\frac{e^2}{mc^2E_g^2W^2}\left[\frac{s^2}{2} + t^2 - \frac{\hbar^2}{m^2}\frac{(s^2k_y^2+4t^2k_z^2)}{E_g^2W^2}\right], \tag{2.6}$$

$$\chi_{so}^{l}(\vec{k}) = \frac{eg\mu_{\mathrm{B}}s^2}{c\hbar E_g^2W^2}\left[\left\{\frac{1-2W}{W} + 4\frac{\hbar^2}{m^2}\frac{t^2(k_x^2+k_y^2)}{E_g^2W^2}\right\}\cos 2\theta^{-} + \left\{\frac{1+2W}{W} - 4\frac{\hbar^2}{m^2}\frac{s^2(k_x^2+k_y^2)}{E_g^2W^2}\right\}\cos 2\theta^{+}\right]$$

$$-2\frac{e^2s^4}{\hbar^2c^2E_g^3W^3}\left[1-2\frac{\hbar^2}{m^2}\frac{s^2(k_x^2+k_y^2)}{E_g^2W^2}\right]$$
$$+\frac{\hbar^2g^2\mu_B^2}{m^2E_g^3W^3}\Big[t^2k_z^2(\cos 2\theta^+ + \cos 2\theta^-)^2$$
$$+\frac{1}{2}s^2(k_x^2+k_y^2)(\cos 2\theta^+ - \cos 2\theta^-)^2\Big], \tag{2.7}$$

and

$$\chi_{so}^t(\vec{k}) = \sqrt{2}\frac{eg\mu_B st}{\hbar cE_g^2W^2}\left[\left\{\frac{W^2+W+1}{W^2}-4\frac{\hbar^2}{m^2}\left(\frac{t^2k_z^2-\frac{1}{2}s^2(k_x^2-k_y^2)}{E_g^2W^2}\right)\right\}\cos^2\theta^+\right.$$
$$\left.-\left\{\frac{W^2-W+1}{W^2}+4\frac{\hbar^2}{m^2}\left(\frac{t^2k_z^2-\frac{1}{2}s^2(k_x^2-k_y^2)}{E_g^2W^2}\right)\right\}\sin^2\theta^-\right]$$
$$-4\frac{e^2s^2t^2}{\hbar^2c^2E_g^3W^3}\left[1-2\frac{\hbar^2}{m^2}\left(\frac{2t^2k_z^2+s^2k_y^2}{E_g^2W^2}\right)\right]$$
$$+\frac{\hbar^2g^2\mu_B^2}{m^2E_g^3W^3}\left[\left\{t^2k_z^2+\frac{1}{2}s^2(k_x^2+k_y^2)\right\}(\cos^2\theta^+-\sin^2\theta^-)^2\right.$$
$$\left.+2s^2k_y^2\cos^2\theta^+\sin^2\theta^-\right]. \tag{2.8}$$

In eqs (2.7) and (2.8), $\sin\theta^\pm$ and $\cos\theta^\pm$ are the amplitudes of single group wave functions in the double group basis states $L_6^\pm(\alpha,\beta)$ [17,12];

$$W = \left[1+2\left(\frac{\hbar^2}{m^2E_g^2}\right)(s^2k_\rho^2+2t^2k_z^2)\right]^{1/2};$$
$$s = \langle L_{61}^+\alpha|\pi^+|L_{62}^-\beta\rangle = \langle L_{61}^+\beta|\pi^-|L_{62}^-\alpha\rangle;$$
$$t = -\langle L_{61}^+\alpha|\pi^z|L_{62}^-\alpha\rangle = \langle L_{61}^+\beta|\pi^z|L_{62}^-\beta\rangle;$$
$$k_\rho^2 = k_x^2+k_y^2;$$

μ_B is the Bohr magneton, g is the Lande g-factor and $\pi^\pm = \frac{1}{\sqrt{2}}(\pi^x \pm i\pi^y)$. The $\vec{k}$ summation is carried out by assuming the Brillouin zone as consisting of four equal spheres and then integrated over the volume of each sphere of radius k_0 equal to $\sqrt{2(m_c+m_v)E_g/\hbar}$ [18], where m_c and m_v are the effective masses of the conduction and valence band edges respectively. The variation of the diamagnetic susceptibility with magnetic impurity concentration is calculated through the change in the energy gap:

$$E_g(x,T) = 190\,\text{meV} + 0.51\frac{(1-9.8x)T^2}{T+56}\,\text{meV K}^{-1}$$
$$+5880x\,\text{meV}; \quad 0\le x\le 0.05 \tag{2.9}$$

for $Pb_{1-x}Eu_xTe$ [13]. We have used the relation defined by eq. (2.9) for our calculation up to $x = 0.06$ for $Pb_{1-x}Eu_xTe$; the error in doing so is not expected to be significant.

Table 1. Various contributions to $\chi_{\rm dia}$ in 10^{-7} emu/gm for p-$Pb_{1-x}Eu_xTe$ at $T = 4.2$ K. The experimental value is taken from ref. [26].

x	χ^l_{ibo}	χ^t_{ibo}	χ_{ibo}	χ^l_{so}	χ^t_{so}	χ_{so}	$\chi_{\rm dia}^{\rm theo.}$	$\chi_{\rm dia}^{\rm expt}$
0.0	−0.157	−0.085	−0.436	−1.324	−0.165	−2.205	−2.643	−3.0
0.03	−0.111	−0.06	−0.308	−0.684	−0.1	−1.179	−1.487	
0.06	−0.082	−0.044	−0.227	−0.408	−0.065	−0.717	−0.944	

B. *Results and discussion*

We present our results for $\chi_{\rm dia}$ in $Pb_{1-x}Eu_xTe$ as a function of x in table 1. We see that both χ_{ibo} and χ_{so} give diamagnetic contributions for small values of x. In all the cases, χ_{so} is much larger than χ_{ibo}, implying the importance of spin-orbit effects in this material. Furthermore, there is considerable anisotropy in both χ_{ibo} and χ_{so}, the longitudinal components being much higher than the transverse ones in each case. The interband anisotropy found in this material is also reflected in a recent calculation of indirect nuclear spin–spin interaction [19]. $\chi_{\rm dia}$ and its constituent terms decrease with increase in x, since the energy gap increases as x increases. The variation of $\chi_{\rm dia}$ with x is indeed remarkable in the sense that the decrease of $\chi_{\rm dia}$ is about 50% for a change in x by about 6%. Unfortunately, barring for the host compound PbTe [4], we are not aware of any experimental result for the alloy system to confirm this trend. However, this is probably justified in the sense that the variation of the band gap $E_g(x)$ is quite appreciable with a positive coefficient as a function of x, as is evident from eq. (2.9) leading to such large changes in $\chi_{\rm dia}(x)$.

3. Local moment magnetization

A. *Contribution due to single ions*

A system of randomly distributed spins in the presence of an external magnetic field $\vec{H}$ is described by the Hamiltonian

$$\mathscr{H} = -g\mu_{\rm B}\vec{H}\cdot\sum_i \vec{S}_i - \sum_{i,j}{}' J_{ij}\vec{S}_i\cdot\vec{S}_j, \tag{3.1}$$

where g is the g-factor of the impurity atom, $\mu_{\rm B}$ is the Bohr magneton, and J_{ij} is the strength of the coupling between spins at sites i and j and is generally assumed to fall off rapidly with separation. In the molecular field approximation, when the field is along the z-direction, we have

$$\mathscr{H} = -g\mu_{\rm B}\sum_i H_{{\rm eff},i}S_{iz}, \tag{3.2}$$

where

$$\mathscr{H}_{{\rm eff},i} = H + \frac{2}{g\mu_{\rm B}}\sum_j{}' J_{ij}\langle S_{jz}\rangle. \tag{3.3}$$

If we neglect the weak long range interaction (second term of eq. (3.3)), the Hamiltonian for an isolated spin is given by

$$\mathscr{H}_s = -g\mu_B S_z H. \tag{3.4}$$

The long range interaction is mainly of indirect exchange type and is expected to be small for the carrier densities, $10^{18}/\text{cm}^3$, for which only, experimental results are available. In the nearest neighbour interaction, a single spin cluster is assumed to have only one magnetic ion surrounded by non-magnetic ions. Thus the short range interaction between the magnetic spins is not considered. If there is one or more nearest neighbours, then the cluster (of connected ions) becomes a multi-spin cluster and the exchange interaction within these clusters (J_p) is considered in the following subsections B and C . The average spin from elementary statistical mechanics can be written as

$$\langle S_z\rangle_s = P_s(x)\frac{\sum_{s=-S}^{S}\{\exp(\beta g\mu_B sH)s\}}{\sum_{s=-S}^{S}\exp(\beta g\mu_B sH)}\ , \tag{3.5}$$

where $P_s(x) = (1-x)^{12}$ for an fcc lattice [20,21]; x is the fraction of ions in the crystal and S is the spin of each magnetic ion. Assuming $y = g\mu_B H/k_B T$, eq. (3.5) can be easily evaluated and is equal to

$$\langle S_z\rangle_s = (1-x)^{12} S B_s(\zeta)\ , \tag{3.6}$$

where

$$B_s(\zeta) = \frac{2S+1}{2S}\coth\left(\frac{2S+1}{2S}\zeta\right) - \frac{1}{2S}\coth\left(\frac{\zeta}{2S}\right) \tag{3.7}$$

and $\zeta = yS$.

B. *Contribution due to two-spin clusters*

The Hamiltonian describing the correlated motion of pairs is

$$\mathscr{H}_p = -g\mu_B(S_{iz}+S_{jz})H - \sum_{\langle ij\rangle}{}' J_{ij}\vec{S}_i\cdot\vec{S}_j\ . \tag{3.8}$$

Assuming an average exchange interaction between identical spins, we have

$$\langle S_z\rangle_p = P_p(x)\frac{\text{Tr}[S_z\exp\{\beta(g\mu_B HS_z + J_p S^2)\}]}{\text{Tr}[\exp\{\beta(g\mu_B HS_z + J_p S^2)\}]}\ , \tag{3.9}$$

where $P_p(x)$ is the probability of finding a pair of impurity spins as nearest neighbours and is equal to $6x(1-x)^{18}$ for an fcc lattice [21]. J_p is the strength of nearest neighbour antiferromagnetic interaction [22]. Noting that the average value of $S^2 = S(S+1)$ and evaluating the trace over the basis $|s\rangle$ as before we write

$$\langle S_z\rangle_p = 6x(1-x)^{18}\frac{\sum_{S_p=0}^{2S_{\max}}\exp\left[\beta J_p S_p(S_p+1)\right]S_p B_{s_p}(\zeta_p)\sinh\left(\frac{2S_p+1}{2S_p}\zeta_p\right)}{\sum_{S_p=0}^{2S_{\max}}\exp\left[\beta J_p S_p(S_p+1)\right]\sinh\left(\frac{2S_p+1}{2S_p}\zeta_p\right)}\,. \tag{3.10}$$

Equation (3.10) is the average spin due to contributions from clusters containing pairs of magnetic ions. $S_{\max}$ is the maximum spin of the pairs, $\zeta_p = yS_p$, S_p being the total spin of a pair.

C. *Contribution due to three-spin clusters*

We consider two types of clusters for the three-spin systems. One is referred to as a 'closed triangle' designated by *ct*, in which each of the magnetic ions is nearest neighbour to the other two. The second type is called an 'open triangle' labelled, *ot* and represents three magnetic ions located on an open string and only one of these ions has two nearest neighbours [21]. Following this reference, we have

$$\langle S_z\rangle_{ct} = P_{ct}(x)\frac{\sum_{S_a=0}^{2S_{\max}}\sum_{S_t=|S_a-S|}^{S_a+S}\exp\left[\beta J_p S_t(S_t+1)\right]S_t B_{s_t}(\zeta_t)\sinh\left(\frac{2S_t+1}{2S_t}\zeta_t\right)}{\sum_{S_a=0}^{2S_{\max}}\sum_{S_t=|S_a-S|}^{S_a+S}\exp\left[\beta J_p S_t(S_t+1)\right]\sinh\left(\frac{2S_t+1}{2S_t}\zeta_t\right)} \tag{3.11}$$

and

$$\langle S_z\rangle_{ot} = P_{ot}(x) \times \frac{\sum_{S_a=0}^{2S_{\max}}\sum_{S_t=|S_a-S|}^{S_a+S}\exp\left\{\beta J_p\left[S_t(S_t+1)-S_a(S_a+1)\right]\right\}S_t B_{s_t}(\zeta_t)\sinh\left(\frac{2S_t+1}{2S_t}\zeta_t\right)}{\sum_{S_a=0}^{2S_{\max}}\sum_{S_t=|S_a-S|}^{S_a+S}\exp\left\{\beta J_p\left[S_t(S_t+1)-S_a(S_a+1)\right]\right\}\sinh\left(\frac{2S_t+1}{2S_t}\zeta_t\right)}, \tag{3.12}$$

where the probabilities of occurrence of these clusters are respectively: $P_{ct}(x) = 8x^2(1-x)^{22}$ and $P_{ot}(x) = 6x^2(1-x)^{23}(7-5x)$, and $\zeta_t = yS_t$. S_t and S_a are the total spin of a triad and any two of the ions in it respectively. The magnetization due to isolated magnetic ions and from two- and three-spin clusters can be written, from eqs (3.6), (3.10), (3.11) and (3.12), as

$$M_i = M_s + M_p + M_{ct} + M_{ot}\,, \tag{3.13}$$

where, in general, $M_\alpha = xN_s g\mu_B\langle S_z\rangle_\alpha$; α stands for *s*, *p*, *ct* and *ot* successively; and N_s is the number of unit cells in the crystal.

D. *Results and discussion*

We present our results of magnetization in table 2 and figures 1 to 3. As expected, the contribution of isolated magnetic ions (M_s) is the dominant one for both $x = 0.03$ and $x = 0.06$.

Table 2. Relative contributions to M for p-type $Pb_{1-x}Eu_xTe$. The experimental values are taken from Gorska *et al* [4].

H (Tesla)	M_s	M_p	M_{ot}	M_{ct}	$M_{\text{tot.}}^{\text{theo.}}$	$M_{\text{tot.}}^{\text{exp.}}$
			$x = 0.03$			
5	2.264	0.565	0.128	0.026	2.984	2.56
10	2.411	0.708	0.185	0.037	3.341	2.80
15	2.435	0.727	0.192	0.039	3.393	2.83
20	2.44	0.731	0.193	0.039	3.403	2.82
			$x = 0.06$			
5	6.559	1.207	0.434	0.092	8.292	7.08
10	6.985	1.603	0.691	0.146	9.426	8.24
15	7.054	1.659	0.732	0.155	9.599	8.40
20	7.067	1.669	0.738	0.156	9.631	8.42

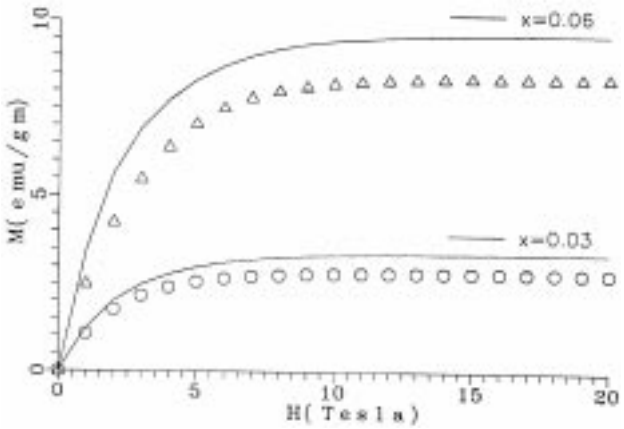

Figure 1. Local moment magnetization versus magnetic field for $Pb_{1-x}Eu_xTe$ for different values of x at 4.2 K. The open circles (○), and triangles (△) represent experimental points for $x = 0.03$ and 0.06 [4], respectively. The solid lines represent our theory.

The contribution decreases as one passes through pairs and triads. The average contributions of pairs and triads are about 30% and 1% respectively of M_s. Thus the contributions from the triads are included only for completeness. However, all the contributions follow the same trend as the field is increased. The contributions from the diamagnetic environment can be calculated from our previous analysis. However, these contributions are quite small and do not affect the overall results in a significant way. Thus there is a magnetic-ion induced phase transformation from diamagnetism to paramagnetism. In calculating M_s for $x = 0.06$, we have relaxed the random approximation for the distribution of isolated ions. This betters the agreement with the experimental results [4]. It may be noted that a new experiment [23] suggests that the magnetic ions are not randomly distributed in the host matrix. But we believe the problem is not yet resolved. We have also not noticed magnetization steps. The agreement with experiment for $x = 0.03$ and 0.06 follows the same

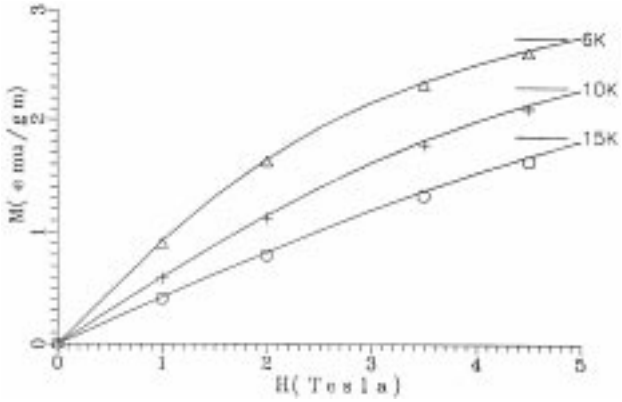

Figure 2. Magnetization versus magnetic field for *p*-type $Pb_{1-x}Eu_xTe$ for $x = 0.03$ at different temperatures. The open circles ($\circ$), plus signs $(+)$ and the triangles ($\triangle$) represent the experimental points for 15 K, 10 K and 6 K respectively [4] and the solid curves represent our theory.

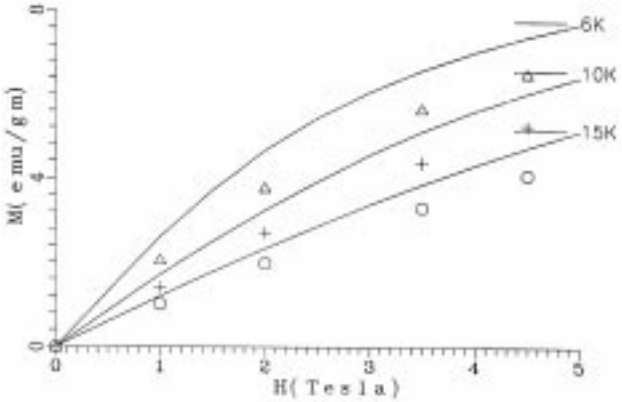

Figure 3. Magnetization versus magnetic field for $Pb_{1-x}Eu_xTe$ for $x = 0.06$ at different temperatures. The open circles ($\circ$), plus signs $(+)$ and the triangles ($\triangle$) represent the experimental points for 15 K, 10 K and 6 K respectively [4] and the solid curves represent our theory.

trend and theoretical values are slightly higher than the experimental ones in both cases. The previous explanations of the magnetization curves involve adjustable parameters [4]. However, we have not used any such parameter. If one looks at table 2, one can find that single-spin contributions are less than experimental values. However, if contributions from the pairs and triads are included, the theoretical values become higher than the experimental values. The discrepancy may be attributed to the following reasons. The interspin interaction is antiferromagnetic in the compound. Therefore, there may be spin-freezing, i.e, the effective number of pairs and triads that actually contribute to the magnetization should be less. However, probability of such frozen spins is actually difficult to calcu-

late. Sometimes, an adjustable parameter, as mentioned earlier, is considered to account for such effects. The other important mechanism that we have not considered is the effect due to bound-spin polarons [2]. We believe inclusion of such effects might improve the agreement. In figures 2 and 3 we have plotted the magnetization contribution as a function of temperature for $x = 0.03$ and $x = 0.06$ respectively. As the temperature is increased, for a given field, the magnetization decreases. The temperature-dependent calculation shows better agreement with experiment [4] for $x = 0.03$ than for $x = 0.06$.

4. Spin-density of carriers

Any calculation of the magnetic properties of degenerate semiconductors is incomplete if the carrier contributions are not considered. The carriers get polarized by both the magnetic field and the localized magnetic ions. However, the magnetic susceptibility of carriers is quite complex and requires separate study. Hence, in what follows, we concentrate on the spin-density of carriers induced by an interaction of type

$$\mathscr{H}_{\text{int}} = \mathscr{H}_{\text{ex}} + \mathscr{H}_z, \tag{4.1}$$

where

$$\mathscr{H}_{\text{ex}} = \frac{1}{2}\sum_{R_i} \mathscr{J}(\vec{r} - \vec{R}_i)\vec{\sigma}\cdot\vec{S}_i \tag{4.2}$$

and

$$\mathscr{H}_z = \frac{1}{2} g_{\text{eff}} \mu_{\text{B}} \vec{\sigma}\cdot\vec{H}\,. \tag{4.3}$$

In eq. (4.2), we have considered only the spin angular momentum because the orbital angular momentum for Eu^{2+} is zero. $\vec{\sigma}$ are Pauli spin matrices, $\mathscr{J}$ describes the strength of this interaction and g_{eff} is the effective g-factor of the carrier [8]. If the field is along z-direction, $\mathscr{H}_{\text{int}}$ is written within a virtual crystal and mean field approximation as

$$\mathscr{H}_{\text{int}} = \frac{1}{2} x N_s \mathscr{J} \langle S_z\rangle \sigma_z + \frac{1}{2} g_{\text{eff}} \mu_{\text{B}} \sigma_z H_z\,. \tag{4.4}$$

We consider the eigenvalue equation

$$\mathscr{H}_t \psi_t = E\,\psi_t, \tag{4.5}$$

where

$$\mathscr{H}_t = \mathscr{H}_0 + \mathscr{H}_{\text{int}}\,, \tag{4.6}$$

and $\mathscr{H}_0$ is the effective mass Hamiltonian for the band edge states [15]. We have from this reference

$$\mathscr{H}_0 \psi_{1,2} = E_2^{-}\psi_{1,2}, \tag{4.7}$$

$$\mathscr{H}_0\psi_{3,4} = E_1^+\psi_{3,4}. \tag{4.8}$$

In eqs (4.7) and (4.8), (ψ_1, ψ_2) and (ψ_3, ψ_4) are the wave functions obtained by diagonalizing the Hamiltonians for the conduction and valence band edge states respectively in the absence of the exchange interaction. These wave functions are given in several of our earlier publications in the subject (see for reference, Hota and Tripathi, [15]). E_2^- and E_1^+ are the corresponding eigenvalues. In order to diagonalize $\mathscr{H}_t$, we use the following matrix elements

$$\langle\psi_3|\mathscr{H}_{\rm int}|\psi_3\rangle = \frac{1}{2}xN_s\langle S^z\rangle X_1\ , \tag{4.9}$$

$$\langle\psi_4|\mathscr{H}_{\rm int}|\psi_4\rangle = -\langle\psi_3|\mathscr{H}_{\rm int}|\psi_3\rangle \tag{4.10}$$

and

$$\langle\psi_3|\mathscr{H}_{\rm int}|\psi_4\rangle = \frac{1}{2}xN_s\langle S^z\rangle X_2, \tag{4.11}$$

where

$$X_1 = \frac{1+W}{2W}A' + 2\frac{\hbar^2}{m^2}\frac{(t^2{k_z}^2 - \frac{1}{2}s^2k_\rho^2)}{E_G^2W(1+W)}B'\ , \tag{4.12}$$

$$A' = A + \frac{g_{\rm eff}\mu_{\rm B}H_z}{xN_s\langle S^z\rangle}\cos 2\theta^+\ , \tag{4.13}$$

$$B' = B - \frac{g_{\rm eff}\mu_{\rm B}H_z}{xN_s\langle S^z\rangle}\cos 2\theta^- \tag{4.14}$$

and

$$X_2 = -4\frac{\hbar^2}{m^2}\frac{tsk_zk_-}{E_G^2W(1+W)}B'\ . \tag{4.15}$$

In eqs (4.13) and (4.14), A and B are the matrix elements of $\sigma^z\mathscr{J}(r)$ between valence and conduction band edge states: $\langle L_{61}^+\alpha|\sigma^z\mathscr{J}(r)|L_{61}^+\alpha\rangle$ and $\langle L_{62}^-\alpha|\sigma^z\mathscr{J}(r)|L_{62}^-\alpha\rangle$ and $k_- = \frac{1}{\sqrt{2}}(k_x - ik_y)$. An exact diagonalization of eq. (4.5) with the help of eqs (4.7) to (4.12) yields two levels for the valance band:

$$E_{\alpha,\beta} = E_1^+ \pm \frac{1}{2}xN_s\langle S^z\rangle\sqrt{X_1^2 + |X_2|^2}\ . \tag{4.16}$$

In order to take into account the effect of far bands we replace E_1^+ in eq. (4.14) by E_V [16]. The magnetization due to holes is calculated using the formula

$$M_c = \mu_{\rm B}(n_\alpha - n_\beta)\ , \tag{4.17}$$

where

$$n_{\alpha,\beta} = \frac{4}{(2\pi)^3}\int \mathrm{d}^3k f(E_{\alpha,\beta} - \mu); \tag{4.18}$$

μ being the Fermi energy for the holes in the p-type $Pb_{1-x}Eu_xTe$ and the factor 4 takes care of all the four valleys. The relative spin density: $(n_\alpha - n_\beta)/(n_\alpha + n_\beta)$ is evaluated numerically and self-consistently involving cylindrical coordinates for the Fermi surface integration in eq. (4.16). The exchange integrals A and B were calculated using experimental parameters [24,6] because the theoretical calculations [25] of these parameters show substantial disagreement with experimental values. The effective g-factors, g_{eff} was calculated using the theory of one of our recent works [8]. In figure 4, we plot the relative spin-density versus x for $p = 10^{18}$ cm^{-3}, $T = 4.2$ K and three values of magnetic fields. With increase in x and H, the spin-density increases, as it should. Notwithstanding the fact that our theory does not work well beyond a carrier density of 10^{18} cm^{-3}, the calculation is first of its kind for this system and reveals interesting results.

5. Summary and conclusion

In this work we make a careful analysis of some magnetic properties of $Pb_{1-x}Eu_xTe$. The quantities considered are lattice diamagnetism, magnetization due to magnetic ions (Eu^{2+}) and spin-density of carriers induced by sp-f hybridization and the magnetic field. We have considered the anisotropy of lattice diamagnetism and show that it is quite pronounced.

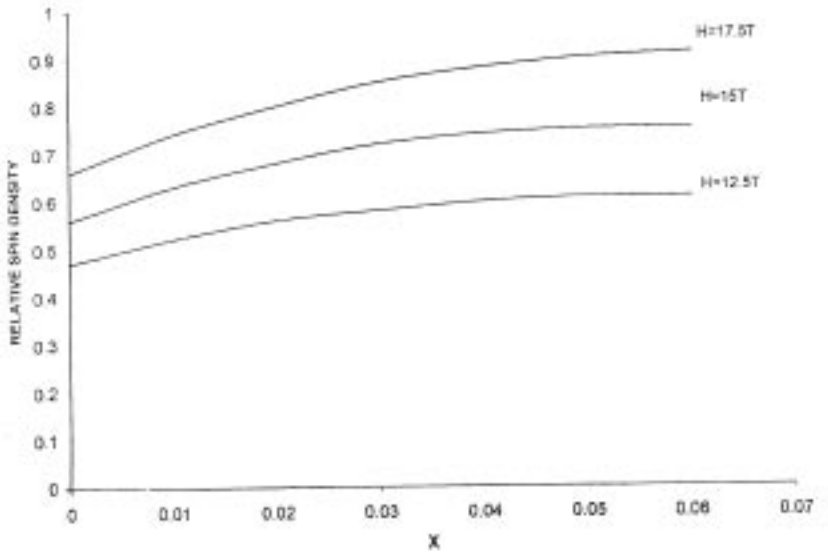

Figure 4. Relative spin-density of carriers for $p = 10^{18}$ cm^{-3} and $T = 4.2$ K as a function of x and magnetic field.

This anisotropy is due primarily to the spin–orbit interaction. The lattice diamagnetism considered in a band model decreases with increase in magnetic ion-concentration. A detailed theoretical analysis of this feature is made for the first time for $Pb_{1-x}Eu_xTe$. Although there are experimental results available for PbTe, we have not come across any other result either due to experimental observation or theoretical evaluation for $Pb_{1-x}Eu_xTe$ for comparison. However, our calculated data, we believe, could be useful for interpreting experimental data.

The magnetization due to magnetic ions is considered independent of surrounding electronic environment. Our results for two typical values of x agree well with the observed field-dependence of magnetization. The agreement has been obtained without any adjustable parameter. We have considered a random distribution of magnetic ions. However, this is relaxed for the contribution from isolated magnetic ions for $x = 0.06$. It may be noted that there is some controversy in the literature as to whether or not the distribution of magnetic ions is random. We believe, on the basis of our results, that the distribution for low concentrations may be random but with increase in x, the ions are probably distributed more regularly. The slightly higher values of theoretically calculated magnetization may probably be due to partial freezing of spins in pairs and triads owing to antiferromagnetic coupling between nearest neighbours.

Finally, we calculated spin-density for carriers in p-type $Pb_{1-x}Eu_xTe$. We emphasize that a detailed theoretical analysis for carrier spin-density for the system is made for the first time. In conclusion, we wish to mention that a serious attempt has been made in this work to incorporate the contributions from the lattice, magnetic ions and charge carriers to different magnetic properties of $Pb_{1-x}Eu_xTe$. Our results compare reasonably well with experimental results where available.

Acknowledgement

One of the authors (GST) acknowledges financial support from UGC, India.

References

[1] J K Furdyna and J Kossut, *Semiconductors and semimetals* (Academic, Boston, 1988) vol. 25
[2] M Averous and M Balkanski (ed.), *Semimagnetic semiconductors and diluted magnetic semiconductors* (Plenum Press, 1991)
[3] G Bauer, H Pascher and W Zawadzki, *Semicond. Sci. Technol.* **7**, 703 (1992)
[4] M Gorska, J R Anderson, G Kido and Z Golacki, *Solid State Commun.* **75**, 363 (1990)
[5] V Bindilatti, N F Oliveira Jr, Y Shapira, G H McCabe, M T Liu, S Iber, S Charar, M Averous, E J McNiff Jr and Z Golacki, *Phys. Rev.* **B53**, 5472 (1996)
[6] S Yuan, H Krenn, G Springholtz, Y Ueta, G Bauer and M Tacke, *Phys. Rev.* **B55**, 4607 (1997)
[7] J M Luttinger and W Kohn, *Phys. Rev.* **97**, 869 (1955)
[8] R C Patnaik and G S Tripathi, *Solid State Commun.* **112**, 669 (1999)
[9] G S Tripathi, *Phys. Lett.* **A115**, 169 (1986); *Phys. Rev.* **B35**, 5247 (1987)
[10] C P Enz, *A course on many-body theory applied to solid state physics* (World Scientfic, Singapore, 1991)
[11] P K Misra and L Kleinman, *Phys. Rev.* **B5**, 4581 (1972)
[12] R L Bernick and L Kleinman, *Solid State Commun.* **8**, 569 (1970)

[13] Shu Yuan, H Krenn, G Springholz and G Bauer, *Phys. Rev.* **B47**, 7213 (1993)
[14] F Geist, W Herbst, C Mejia-Garcia, H Pascher, R Rupprecht, Y Ueta, G Springholtz, G Bauer and M Tacke, *Phys. Rev.* **B56**, 13042 (1997)
[15] R L Hota and G S Tripathi, *J. Phys. Condens. Matter* **3**, 6299 (1991)
[16] R L Hota, G S Tripathi and J N Mohanty, *Phys. Rev.* **B47**, 9319 (1993)
[17] D L Mitchell and R F Wallis, *Phys. Rev.* **151**, 581 (1966)
[18] L Liu, *Phys. Rev.* **B26**, 975 (1982)
[19] R C Patnaik, R L Hota and G S Tripathi, *Phys. Rev.* **58**, 3924 (1998)
[20] R E Behringer, *J. Chem. Phys.* **29**, 537 (1958)
[21] R R Galazka, S Nagata and P H Keesom, *Phys. Rev.* **B22**, 3344 (1980)
[22] J R Anderson and M Gorska, *Solid State Commun.* **52**, 601 (1984)
[23] E ter Haar, B Bindilatti, N F Oliveira Jr, G H McCabe, Y Shapira, Z Golacki, S Charar, M Averous and E J McNiff Jr, *Phys. Rev.* **B56**, 8912 (1997)
[24] G Karczewski, J K Furdyna, D L Partin, C N Thrush and J P Herman, *Phys. Rev.* **B46**, 13331 (1992)
[25] T Dietl, C Sliwa, G Bauer and H Pascher, *Phys. Rev.* **B55**, 2230 (1994)
[26] M Gorska and J R Anderson, *Acta Physica Polonica* **A75**, 273 (1989)